The Canadian Mineralogist
Vol. 35, pp. 201-216 (1997)

SHORT-RANGE ORDER IN AMPHIBOLES: A BOND-VALENCE APPROACH

FRANK C. HAWTHORNE*

CNR-Centro di Studio per la Cristallochimica e la Cristallografia, via Abbiategrasso 209, I-27100 Pavia, Italy

ABSTRACT

Short-range order describes the tendency for some local arrangements of atoms to be more frequent than a random distribution of atoms would indicate. Bond-valence theory indicates that local arrangements that closely obey the valence-sum rule should be more stable, and hence favored, over arrangements that lead to significant departures from the valence-sum rule. This argument should be particularly effective in predicting local arrangements in amphiboles because of the wide dispersion of bond valences associated with the different heterovalent site-occupancies characteristic of ideal end-members of the amphibole group. Of the amphibole end-member charge-arrangements, only tremolite, glaucophane, (alumino-)leakeite and ungarettiite have ordered distributions of cations; all other end-members involve disorder on two or more cation sites, affording extensive possibilities for short-range order. Here, the most probable patterns of short-range order have been derived for all monoclinic calcic, sodic–calcic and alkali amphiboles by examining local bond-valence distributions and their agreement with the valence-sum rule. For most structures, there is one set of patterns that agrees quite well with the valence-matching principle, and all other sets of patterns show significant deviations from the valence-matching principle. For some structures, one pattern of the best set of patterns of order deviates significantly from the valence-sum rule (*e.g.*, tschermakite), and compositions close to these end-members are rare or non-existent. These patterns of local order will hopefully aid in the interpretation of experimental data, which are affected significantly by short-range order in the amphibole structure.

Keywords: amphibole, short-range order, bond-valence theory.

SOMMAIRE

Le concept d'ordre à courte échelle décrit la tendance qu'ont certains agencements locaux d'atomes d'être plus courants qu'une distribution aléatoire d'atomes le prédirait. La théorie des valences de liaison prédit que les arrangements locaux qui concordent étroitement avec la règle des sommes des valences devraient être plus stables, et donc favorisés, en comparaison des arrangements qui mènent à des écarts importants de cette règle. Cet argument devrait être particulièrement efficace pour prédire les arrangements locaux dans les amphiboles, à cause de la grande dispersion des valences de liaison associées aux divers schémas d'occupation hétérovalente des sites des pôles idéaux qui constituent la famille des amphiboles. Parmi les pôles d'amphiboles pouvant contenir l'agencement Na–Mg–Al, seuls trémolite, glaucophane, (alumino)leakeïte et ungarettiite contiennent une distribution ordonnée des cations. Tous les autres pôles impliquent un certain désordre dans au moins deux sites de cations, ce qui explique la multiplicité de possibilités de mise en ordre à courte échelle. Dans ce travail, les schémas les plus probables d'ordre local ont été dérivés pour toutes les amphiboles monocliniques calciques, sodiques–calciques et alcalines par examen de leurs distributions locales des valences de liaison et leur concordance avec la règle des sommes des valences. Dans la plupart des structures, il y a une seule façon de distribuer les cations de sorte que le principe de concordance des valences de liaison soit respecté; tous les autres agencements démontrent des écarts importants à ce principe. Pour certaines structures, par exemple la tschermakite, un agencement parmi les meilleurs agencements ordonnés dévie de façon importante à la règle, et les compositions voisines de ces pôles sont effectivement rares ou inconnues. Il est à souhaiter que ces schémas d'agencement ordonnés locaux servent à mieux interpréter les résultats expérimentaux, dans lesquels les effets d'ordre local dans la structure de l'amphibole s'avèrent importants.

(Traduit par la Rédaction)

Mots-clés: amphibole, ordre à courte échelle, théorie des valences de liaison.

INTRODUCTION

The amphibole structure (Fig. 1) is one of great structural compliance; it can incorporate a wide variety of cations from monovalent to tetravalent, and from small (Si: $^{[4]}r = 0.26$ Å) to large (Rb: $^{[12]}r = 1.72$ Å; Shannon 1976). Thus the structure can respond to differences in rock composition and differences or changes in conditions of crystallization or equilibration, with the result that amphiboles are rock-forming minerals in a wide variety of parageneses. Knowledge of the site populations and order–disorder relations in amphiboles is

* Occasionally at the Department of Geological Sciences, University of Manitoba, Winnipeg, Manitoba R3T 2N2. *E-mail address*: fchawthorn@bldgwall.lan1.umanitoba.ca

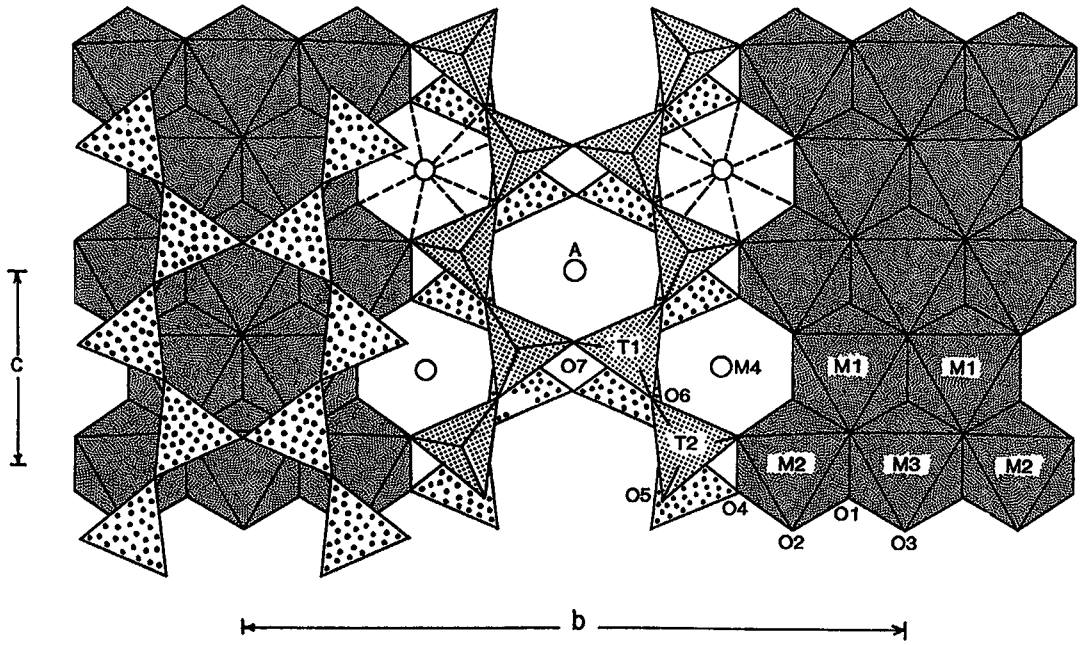

FIG. 1. The *C2/m* amphibole structure projected onto (100).

essential to our understanding of amphibole crystal-chemistry, physical properties and thermodynamic behavior, and the amphiboles, more than any other group of minerals, have been the focus of site-occupancy studies (Hawthorne 1981a, 1983). Extensive spectroscopic work has been done on the amphiboles (Hawthorne 1981b). However, in most cases, the chemical and structural complexity of the amphiboles has prevented significant work. Only for simple compositions (*e.g.*, cummingtonite–grunerite: Hafner & Ghose 1971; anthophyllite: Seifert 1978) have useful results been obtained, although spectroscopic methods have proved quite powerful in studies of synthetic amphiboles [Della Ventura (1992), and references therein]. Most of the information on cation order in amphiboles has been produced by crystal-structure refinement. Although certain important issues still remain obscure (*e.g.*, the general behavior of Ti and Mn), we now have a reasonably comprehensive knowledge of patterns of long-range order in amphiboles.

LONG-RANGE ORDER AND SHORT-RANGE ORDER

There are two types of order, LRO (Long-Range Order) and SRO (Short-Range Order). Long-range order describes site occupancies, the amount of a species at a particular site in the structure, averaged over the whole crystal; thus in a specific amphibole, the LRO gives the *average* site-occupancies, *e.g.*, $M(1) = 0.52Mg + 0.48Fe^{2+}$, $M(2) = 0.38Mg + 0.62Fe^{2+}$, $M(3) = 0.48Mg + 0.52Fe^{2+}$. Short-range order describes the *local* association of species at adjacent (usually NNN, Next-Nearest Neighbor) sites in the structure. Thus in the amphibole considered above, SRO describes the tendency of Mg and Fe to associate in *local* clusters (MgMgMg, MgMgFe, MgFeFe, FeFeFe); in a short-range disordered structure, these local arrangements occur in proportions concordant with a random distribution, whereas in a short-range ordered structure, some arrangements are more frequent than others, *relative to a random distribution.* Crystal-structure refinement gives a long-range view of the amphibole structure, and has been of particular importance in furthering our understanding of amphibole chemistry. However, it provides no *direct* information on SRO. This is a significant drawback, as SRO can have many important effects in minerals. For example, (1) SRO can affect structural and chemical variations in rock-forming minerals (*e.g.*, staurolite: Hawthorne *et al.* 1993a; tourmaline: Hawthorne 1996) and can lead to nonlinear relations between structural and chemical variables (*e.g.*, amphiboles: Hawthorne *et al.* 1996a). (2) SRO can contribute significantly to a reduction of configurational entropy in solid solutions, and is important in considerations of configurational entropy and the formulation of activity models for complex

rock-forming silicates (*e.g.*, amphiboles: Graham & Navrotsky 1986, Jenkins 1988, 1994, Pawley *et al.* 1993, Smelik *et al.* 1994).

Characterization of Short-Range Order

The characterization of SRO is quite difficult. In principle, this can be done by diffraction (*i.e.*, scattering) methods; however, the information on SRO tends to be overwhelmed by information from the rest of the structure, and little work of this type has been done on minerals. Spectroscopic techniques are, in principle, better suited to the characterization of SRO, as they focus on a specific (energetic) aspect of a structure, rather than recording all information about the structure. In hydroxyl-amphiboles, information on SRO can, in principle, be obtained *via* infrared spectroscopy in the principal OH-stretching region (Strens 1966, 1974, Law 1976, Hawthorne *et al.* 1996b, c), and this has been done for synthetic amphiboles of simple composition (Della Ventura *et al.* 1996a, b, c, d). X-ray absorption spectroscopy (XAS) and Magic-Angle-Spinning Nuclear Magnetic Resonance (MAS NMR) also can be used to determine SRO, and work on minerals is currently in progress.

When using spectroscopic techniques to characterize SRO, one must be able to assign all of the spectral features to specific local configurations, and then the relative intensities of the spectral bands give the relative abundance of each configuration (subject to corrections for possible variation in transition moment among the bands). In order to do this, one must have a good starting model; one must know the possible stable local arrangements, and one must know their relative spectroscopic signals. As one is testing models rather than deriving an *ab initio* solution, it is important that the model to be tested is comprehensive and physically realistic. The same argument applies to the use of short-range order arguments in crystal chemistry and thermodynamics; one must begin with the correct model, or any further arguments will be wrong.

Bond-Valence Theory

Brown (1981, 1992) has developed a simple approach to chemical bonding in inorganic structures based on the empirical bond-valence curves of Brown & Shannon (1973). A crystal is considered as an array of atoms connected by a network of chemical bonds. For oxide and oxysalt minerals, any path through this network consists of alternating cations and anions, and the total network is subject to the law of electroneutrality: the total valence of the cations is equal to the total valence of the anions. Bond-valence is a measure of the strength of a chemical bond, and can be calculated from the curves of Brown & Shannon (1973) and Brown & Altermatt (1985) if the bond lengths are known. The valence-sum rule states that *the sum of the bond-valences incident at each atom is equal to the magnitude of the formal valence of that atom.* If the interatomic distances are not known, the bond-valences can be approximated by the Pauling bond-strengths (Pauling 1929). Bond-valence arguments are usually applied to the long-range aspects of a structure. However, this is not an intrinsic restriction of this approach. Burdett & Hawthorne (1993) have shown that the bond-valence – bond-length relation may be derived algebraically from a molecular-orbital description of a solid in which there is a significant energy-gap between the interacting orbitals on adjacent atoms. Bond-valence theory may thus be considered as a very simple form of molecular-orbital theory, parameterized *via* interatomic distance and scaled *via* the valence-sum rule. Hence it may be used to characterize SRO in a structure in much the same way as it has been used to characterize LRO, with the exception that the true interatomic distances are not known, and the local bond-valences must be approximated where long-range disorder is present in the structure.

The valence-sum rule does not hold exactly, and one cannot give a realistic universal limiting value of agreement beyond which a structure is not stable, as such values seem to be structure-dependent. For the amphibole structure, the O(4) anion usually shows bond-valence sums in the range 1.80–1.90 *vu* (valence units), whereas the bond-valence sums for the other anions are in the range 1.85–2.15 *vu* (or, more usually, 1.90–2.10 *vu*). I use these values here, although it must be stated that they are somewhat subjective.

It is perhaps worthwhile emphasizing explicitly that bond-valence constraints tend to minimize the enthalpy of the crystal. They are not sufficient to define the atomic arrangement exactly, but they provide strong constraints on both cation and anion order and on variation in bond lengths. This is in accord with the fact that the Gibbs free energy is also affected by configurational entropy, and it is now thought that configurational entropy arising from long-range disorder plays a major role in stabilizing amphiboles at high temperature (Hawthorne 1995). However, there is accumulating evidence (Della Ventura *et al.* 1996d) that long-range disorder can be accompanied by extensive short-range order.

Ordered Amphiboles

It is important to characterize the bond-valence patterns in ordered amphiboles, as the true interatomic distances are known, and the bond-valences can be calculated from the bond-valence curves of Brown & Shannon (1973) and Brown & Altermatt (1985). These bond-valence patterns give an indication of the type of bond valences expected in amphiboles, and help to approximate the bond-valence patterns for atomic distributions involving SRO, where the bond lengths are not known. The only ordered amphibole end-members

are tremolite, glaucophane, leakeite and ungarettiite; their bond-valence arrangements are shown in Table 1.

Tremolite

The arrangement for tremolite, $\square Ca_2Mg_5Si_8O_{22}(OH)_2$, is calculated from the structure of Papike *et al.* (1969). The *M*(1)–O and *M*(3)–O bond-valences are all close to 0.333, the Pauling bond-strength, whereas the *M*(2)–O and *M*(4)–O bond-valences show considerable dispersion about the Pauling bond-strengths, reflecting the influence of the O(4) anion that is only [3]-coordinated and hence is involved in very short bonds. The sum of the bond-valence incident at O(4) is 1.84 *vu*, significantly less than the ideal value of 2.00 *vu*. This low sum at O(4) is characteristic of the amphibole (and pyroxene) structures (Hawthorne 1983); it presumably represents local strain in the structure (Brown 1992), and indicates that a bond-valence sum of ~1.80 *vu* at O(4) (but not at other anions) is acceptable in the amphibole structure. The O(5) and O(6) anions also are [3]-coordinated in tremolite, but both are linked to two Si atoms at *T*(1) and *T*(2), and the sum of the incident Pauling bond-strengths significantly exceeds 2.00 *vu*. To compensate for this fact, the bond-lengths from *T*(1), *T*(2) and *M*(4) to O(5) and O(6) are significantly longer than the mean values for the *T*(1), *T*(2) and *M*(4) polyhedra, and the corresponding bond-valences (Table 1) are less than the analogous Pauling bond-strengths. With this general model in mind, *local* bond-valence arrangements for possible short-range-ordered arrangements can be constructed for long-range-disordered amphibole end-members.

TABLE 1. BOND-VALENCE TABLES FOR THE ORDERED AMPHIBOLES TREMOLITE, GLAUCOPHANE, ALUMINO-LEAKEITE AND UNGARETTIITE

Tremolite

	M(1)	*M*(2)	*M*(3)	*M*(4)	*A*	*T*(1)	*T*(2)	Σ
O(1)	0.36$^{\times 2}\downarrow$	0.31$^{\times 2}\downarrow$	0.35$^{\times 1}\downarrow$			1.05		2.07
O(2)	0.34$^{\times 2}\downarrow$	0.34$^{\times 2}\downarrow$		0.29$^{\times 2}\downarrow$			1.00	1.97
O(3)	0.34$^{\times 2}\downarrow\rightarrow$		0.36$^{\times 2}\downarrow$					1.04
O(4)		0.40$^{\times 2}\downarrow$		0.34$^{\times 2}\downarrow$			1.10	1.84
O(5)				0.13$^{\times 2}\downarrow$	–	0.97	0.93	2.03
O(6)				0.21$^{\times 2}\downarrow$	–	0.98	0.91	2.10
O(7)					–	1.02$^{\times 2}\rightarrow$		2.04
Σ	2.08	2.10	2.12	1.94	–	4.02	3.94	

Glaucophane

	M(1)	*M*(2)	*M*(3)	*M*(4)	*A*	*T*(1)	*T*(2)	Σ
O(1)	0.35$^{\times 2}\downarrow$	0.38$^{\times 2}\downarrow$	0.34$^{\times 1}\downarrow$			1.01		2.08
O(2)	0.35$^{\times 2}\downarrow$	0.47$^{\times 2}\downarrow$		0.18$^{\times 2}\downarrow$			1.01	2.01
O(3)	0.34$^{\times 2}\downarrow\rightarrow$		0.36$^{\times 2}\downarrow$					1.04
O(4)		0.59$^{\times 2}\downarrow$		0.21$^{\times 2}\downarrow$			1.08	1.88
O(5)				0.10$^{\times 2}\downarrow$	–	1.02	0.96	2.08
O(6)				0.17$^{\times 2}\downarrow$	–	1.00	0.92	2.09
O(7)					–	1.03$^{\times 2}\rightarrow$		2.06
Σ	2.08	2.88	2.04	1.32	–	4.06	3.95	

Alumino-Leakeite

	M(1)	*M*(2)	*M*(3)	*M*(4)	*A**	*T*(1)	*T*(2)	Σ
O(1)	0.28$^{\times 2}\downarrow$	0.46$^{\times 2}\downarrow$	0.16$^{\times 1}\downarrow$			1.10		2.00
O(2)	0.30$^{\times 2}\downarrow$	0.44$^{\times 2}\downarrow$		0.16$^{\times 2}\downarrow$			1.10	2.00
O(3)	0.42$^{\times 2}\downarrow\rightarrow$		0.17$^{\times 2}\downarrow$					1.01
O(4)		0.60$^{\times 2}\downarrow$		0.20$^{\times 2}\downarrow$			1.10	1.90
O(5)				0.04$^{\times 2}\downarrow$	0.18$^{\times 2}\downarrow$	1.00	0.90	2.12
O(6)				0.10$^{\times 2}\downarrow$	0.12$^{\times 2}\downarrow$	1.00	0.90	2.12
O(7)					0.20$^{\times 2}\downarrow$	0.90$^{\times 2}\rightarrow$		2.00
Σ	2.00	3.00	0.98	1.00	1.00	4.00	4.00	

Ungarettiite

	M(1)	*M*(2)	*M*(3)	*M*(4)	*A**	*T*(1)	*T*(2)	Σ
O(1)	0.31$^{\times 2}\downarrow$	0.27$^{\times 2}\downarrow$	0.44$^{\times 1}\downarrow$			1.04		2.06
O(2)	0.56$^{\times 2}\downarrow$	0.32$^{\times 2}\downarrow$		0.17$^{\times 2}\downarrow$			0.98	2.03
O(3)	0.60$^{\times 2}\downarrow\rightarrow$		0.61$^{\times 2}\downarrow$					1.81
O(4)		0.45$^{\times 2}\downarrow$		0.18$^{\times 2}\downarrow$			1.15	1.78
O(5)				0.07$^{\times 2}\downarrow$	0.18$^{\times 2}\downarrow$	1.02	0.91	2.09
O(6)				0.14$^{\times 2}\downarrow$	0.10$^{\times 2}\downarrow$	1.02	0.90	2.11
O(7)					0.15$^{\times 2}\downarrow$	0.98$^{\times 2}\rightarrow$		2.11
Σ	2.94	2.08	2.98	1.12	0.86	4.06	3.94	

* see discussion on the *A* site in the text.

Glaucophane

Glaucophane, $\square Na_2(Mg_3Al_2)Si_8O_{22}(OH)_2$, is a completely ordered end-member amphibole, with $M(4) = Na_2$, $M(1) = Mg_2$, $M(2) = Al_2$, $M(3) = Mg_1$ and $T(1) = T(2) = Si_4$. The bond-valence arrangement is calculated from the intermediate-composition glaucophane structure of Papike & Clark (1968), and the bond-valences have been adjusted slightly to conform to an ideal end-member composition. The features of the bond-valence sums incident at the anions are very similar to those in tremolite, despite the differences in chemical composition.

Leakeite

Ideal "alumino-leakeite", $NaNa_2(Mg_2Al_2Li)Si_8O_{22}(OH)_2$ (*cf.* leakeite, Hawthorne *et al.* 1992, 1994), has $M(1) = Mg_2$, $M(2) = Al_2$ and $M(3) = Li$ and hence is ordered, with only one possible arrangement (Table 1). Attempts to put Li at any other site in an amphibole of this composition results in considerable deviations from the valence-sum rule.

Ungarettiite

Ungarettiite, $NaNa_2(Mn^{2+}_2Mn^{3+}_3)Si_8O_{22}O_2$ (Hawthorne *et al.* 1995), has $M(1) = Mn^{3+}_2$, $M(2) = Mn^{2+}_2$, $M(3) = Mn^{3+}$ and $O(3) = O^{2-}_2$, and hence is ordered with only one possible arrangement (Table 1). The occurrence of O^{2-} at O(3) requires coordination of the O(3) anion by three trivalent cations, and the above arrangement satisfies this requirement. Even with this pattern of order, the O(3)–Mn^{3+} bond-lengths must be strongly shortened relative to the <Mn^{3+}–O> bond-lengths, and this arrangement may only be possible with Mn^{3+}, which normally has short axial bonds owing to Jahn–Teller instability (Jahn & Teller 1937, Burns *et al.* 1994).

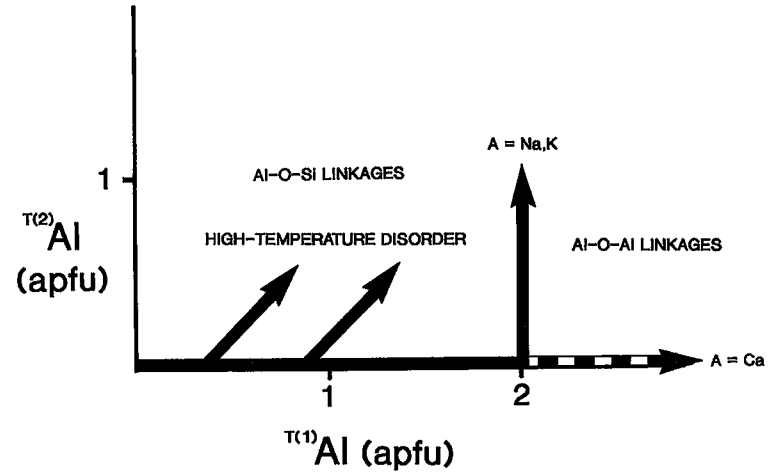

FIG. 2. Types of long-range order of [4]Al in *C2/m* amphiboles; the horizontal and vertical thick lines denote the usual pattern of order in low- and medium-temperature amphiboles containing ^{A}(Na,K,□), the diagonal thick lines denote high-temperature disorder of [4]Al between *T*(1) and *T*(2), and the broken line denotes the pattern of [4]Al order in ^{A}Ca-bearing amphiboles [modified from Oberti *et al.* (1995b)].

Al–Si ORDER IN THE CHAIN OF TETRAHEDRA

Long-range order

Long-range aspects of Al and Si order over the *T*(1) and *T*(2) sites were treated in detail by Oberti *et al.* (1995b). Generally, where [4]Al < 2 atoms per formula unit (*apfu*), [4]Al is ordered at the *T*(1) site; where [4]Al > 2 *apfu*, 2 *apfu* of [4]Al occurs at *T*(1) and all [4]Al in excess of 2 *apfu* is ordered at *T*(2). This situation is somewhat sensitive to conditions of crystallization. Oberti *et al.* (1995b) showed that amphiboles from high-temperature environments have [4]Al partly disordered over *T*(1) and *T*(2) where [4]Al < 2 *apfu*. The ordering of [4]Al, first into *T*(1) and then into *T*(2), in low- and medium-temperature environments, is due to the need to avoid Al–O–Al linkages that are unfavorable from a local bond-valence viewpoint (Oberti *et al.* 1995b). This picture of the behavior of [4]Al was extended by the recent discovery of a new amphibole species, fluor-cannilloite, ideally $CaCa_2(Mg_4Al)(Si_5Al_3)O_{22}F_2$ (Hawthorne *et al.* 1996d). In this amphibole, all [4]Al is ordered at the *T*(1) site, and Al–O–Al linkages *must* occur; indeed, it is the occurrence of Al–O–Al linkages that drives the incorporation of Ca at the *A* site. The patterns of long-range order of [4]Al are summarized in Figure 2, together with the occurrence of Si–O–Al and Al–O–Al linkages *required* by specific patterns of order.

Next, we will briefly consider the factors affecting *T*–O–*T* linkages in amphiboles in which *T* represents Si,Al. Where a *T*–O–*T* linkage is Si–O–Al, the sum of the incident bond-valences at the oxygen anion is ~1.75 *vu*. For the O(5) and O(6) anions, the bond-valence requirements of the anion are easily satisfied by bonds from the *M*(4) and *A* cations. For the O(7) anion, the situation is somewhat different, as O(7) bonds only to *T*(1) (twice) and *A*, with a small contribution from a hydrogen bond where O(3) = OH (Hawthorne 1983). The *T*(1)–O(7) bonds can shorten somewhat to increase the bond-valence incident at O(7), an effect that can be combined with lengthening of one or more of the other *T*(1)–O bonds, but O(7) has much less flexibility in this regard than the O(5) and O(6) anions. The principal part of the bond-valence deficiency at O(7) caused by an Si–O–Al linkage is compensated by Na or K at the *A* site (Hawthorne 1983, Hawthorne *et al.* 1996a). Thus where A = □, the structure has difficulty in satisfying the local bond-valence requirement at the O(7) anion, accounting for the fact that tschermakitic amphiboles are uncommon. Where a *T*–O–*T* linkage is Al–O–Al, the sum of the incident bond-valences at the central anion is ~1.50 *vu*. The bond-valences of *M*(4)–O(5) and *M*(4)–O(6) bonds in typical amphibole structures are shown in Table 2, together with corresponding *A*–O(5) and *A*–O(6) bond-valences. In no case can the incident bond-valence at O(5) and O(6) compensate for the low bond-valence incident from the *T* cations in an Al–O–Al linkage. The situation is the same for the O(7) anion (Table 2); even though *A*–O(7) is the shortest *A*–O bond by far, the O(7) bond-valence requirements cannot be satisfied for an Al–O–Al linkage and *A* = Na,K.

TABLE 2. BOND-VALENCES* INCIDENT AT THE O(5), O(6) AND O(7) SITES FROM THE *M*(4) AND *A* CATIONS IN SELECTED AMPHIBOLES

	(1)	(2)	(3)	(4)
O(5)–*M*(4)	0.130	0.080	0.179	0.167
O(5)–*A*	0.073	0.154	0.065	0.124
Σ	0.203	0.234	0.244	0.291
O(6)–*M*(4)	0.185	0.133	0.204	0.183
O(6)–*A*	0.055	0.047	0.095	0.107
Σ	0.240	0.180	0.299	0.290
O(7)–*A*	0.169	0.179	0.210	0.171

(1) Potassian ferri-taramite (Hawthorne & Grundy 1978);
(2) Potassian arfvedsonite (Hawthorne 1976);
(3) Potassian pargasite (Robinson *et al.* 1973);
(4) Magnesio-hastingsite (Bocchio *et al.* 1978)

* calculated from the curves of Brown (1981)

However, if A = Ca, the short A–O(7) distance of 2.4 Å (Hawthorne *et al.* 1996d) allows Ca to contribute sufficient bond-valence to satisfy the anion bond-valence requirements of an Al–O–Al linkage through O(7). Hence Al–O–Al linkages can occur, where A = Ca, and do occur in fluor-cannilloite, where all $^{[4]}$Al is ordered at T(1) (Hawthorne *et al.* 1996d). This behavior is also indicated in Figure 2. Calcium, Na and K are ordered at the off-centered A(2) and $A(m)$ sites, and the implications of this fact are discussed in the next section.

Short-range order

Above, I have summarized the patterns of long-range order of $^{[4]}$Al in amphiboles, and have explained this in terms of a short-range mechanism, the satisfaction of local bond-valence requirements. Now, we will examine the short-range configurations associated with these patterns of order. Figure 3 shows a series of patterns of order in the double chain of tetrahedra; these patterns are concordant with the long-range behavior of Figure 2. For a composition, $T = Si_8$, the chain is completely long-range and short-range ordered (Fig. 3a). For $T = Si_6Al_2$ with $T(1) = Si_2Al_2$, every pair of T(1) sites is occupied by Si–Al, but there is potential for order–disorder in terms of the sequence (Al–Si or Si–Al) in adjacent pairs of T(1) sites (Fig. 3b). Where $T = Si_5Al_3$ and Al–O–Al linkages are not allowed, T(1) contains Si_2Al_2, T(2) contains Si_2Al, and each $^{T(2)}$Al occurs in a hexagonal ring (of tetrahedra) with two T(1) = Al tetrahedra to which it is *not* linked (Fig. 3c); this configuration has two possible orientations, and hence a degree of disorder is still possible within an individual double-chain. Where $T = Si_4Al_4$ and Al–O–Al linkages are not allowed (Fig. 3d), both T(1) and T(2) must be Si_2Al_2, and the chain is completely ordered and loses its long-range mirror symmetry; any disruption of this pattern of order forces an Al–O–Al linkage. Of course, adjacent double-chains can be orientationally disordered, and long-range $C2/m$ symmetry need not be broken by such order within the double-chain of tetrahedra. Where $T = Si_5Al_3$ and $T(2) = Si_4$ are present, Al–O–Al linkages are allowed (Fig. 3e), and a significant degree of order–disorder is involved in the sequence of Al–Al, Si–Al and Al–Si pairs along the length of the chain. Where $T = Si_4Al_4$ and $T(2) = Si_4$ are present, all T(1)–O(7)–T(1) linkages are Al–O–Al (Fig. 3f), and the chain is completely ordered. Furthermore, the patterns of order in symmetry-equivalent chains are also identical, and so there is no disorder associated

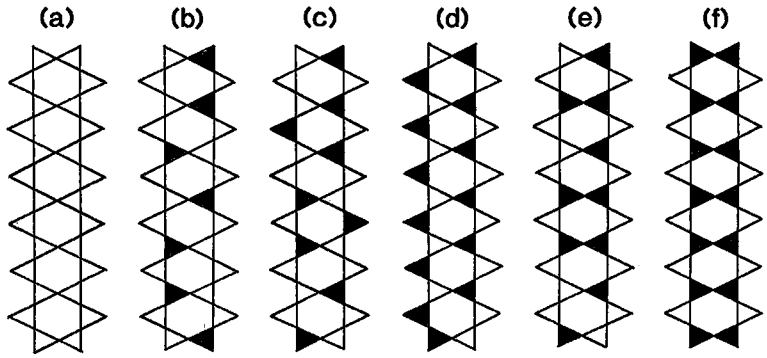

FIG. 3. Patterns of order in double chains of tetrahedra having different composition and different T–O–T linkages, in which $^{[4]}$Al-containing tetrahedra are colored black: (a) $T = Si_8$; (b) $T = Si_6Al_2$, $T(1) = Si_2Al_2$ with no Al–O–Al linkages; (c) $T = Si_5Al_3$, $T(1) = Si_2Al_2$ with no Al–O–Al linkages; (d) $T = Si_4Al_4$, $T(1) = Si_2Al_2$ with no Al–O–Al linkages; (e) $T = Si_5Al_3$, $T(1) = SiAl_3$ with Al–O–Al linkages; (f) $T = Si_4Al_4$, $T(1) = Al_4$ with Al–O–Al linkages.

with different chains, as occurs wherever the double chain does not completely obey the full symmetry of the crystal.

The patterns of order in Figure 3 give us a general framework within which to consider the patterns of short-range order that are both possible and probable in amphiboles of intermediate composition.

Coupling Between *A* and *T* Cations

There are two factors that affect the patterns of order of the *A* cations in the *A* cavity of the amphibole structure: (1) Na, K and Ca cannot occupy the *A2/m* site, as their bond-valence requirements cannot be satisfied at this site (Hawthorne 1983); (2) local disorder of the *A* cations is coupled to the bond-valence requirements of the O(5), O(6) and O(7) anions, which are, in turn, affected directly by the occupancy of the *T*(1), *T*(2) and *M*(4) sites (Hawthorne *et al.* 1996a). We may investigate the geometrical aspects of the latter effect by considering the pargasite chain (Fig. 3b) and combining it with configurations of local order at the *A* site. The *A* site is surrounded by twelve tetrahedra arranged in two parallel hexagonal rings that are each part of different double-chains (Fig. 4a). Each linked pair of *T*(1) tetrahedra can be occupied by Al and Si, and so there are

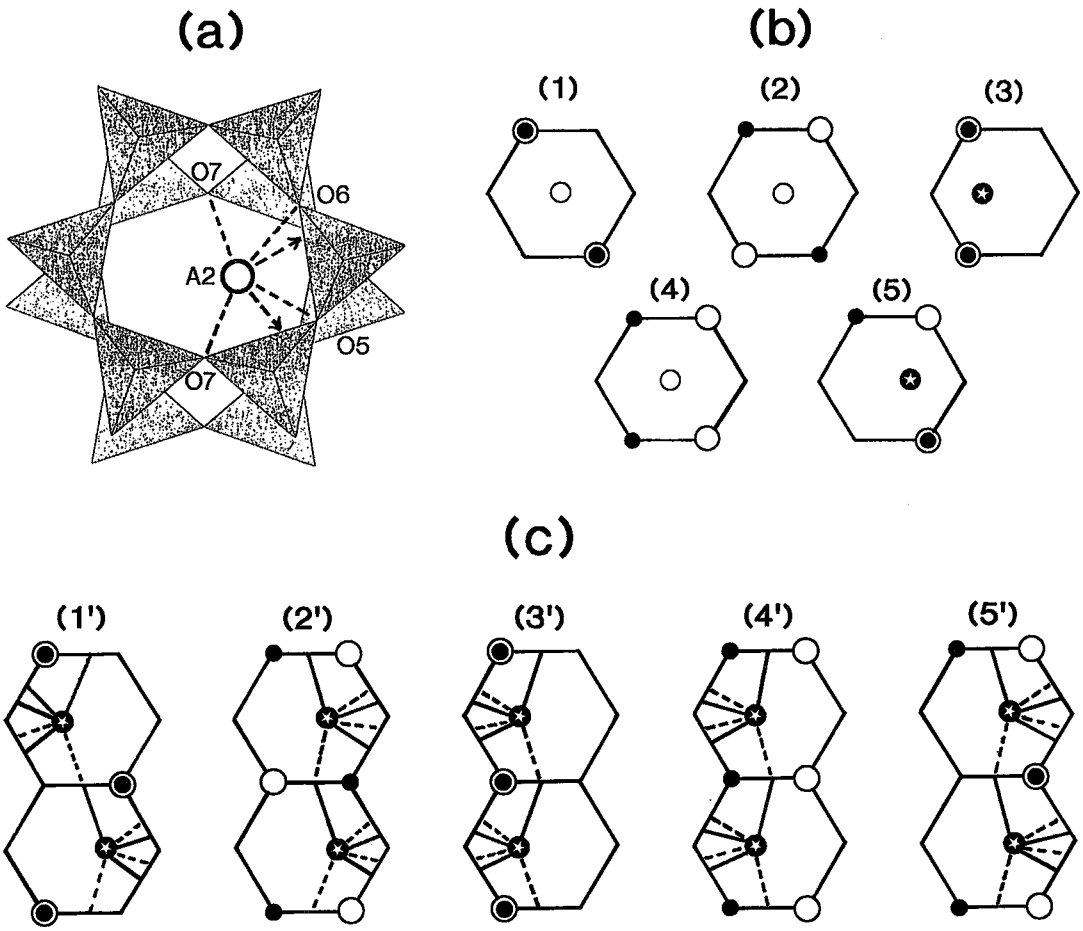

FIG. 4. Details of short-range order of $^{T(1)}$Al and $^{A(2)}$Na around the *A* cavity in pargasite; bonds to O(5), O(6) and O(7) anions are shown by broken lines (upper hexagonal ring) and full lines (lower hexagonal ring): (a) the *A* cavity surrounded by two hexagonal rings of *T*(1) and *T*(2) tetrahedra, with the *A*(2) site indicated by a hollow sphere; (b) graphs of the arrangement in (a); lines denote linkage between tetrahedra, upper and lower hexagonal rings are superimposed; Si atoms are not shown, Al atoms are shown by black circles (upper ring) and hollow circles (lower ring); the *A*(2) cation is shown by a starred circle, and the *A*(2/*m*) position is shown by the hollow circle; (c) possible conformations in adjacent cavities involving the arrangements of Figure 4b.

several different arrangements of Al cations over the tetrahedra surrounding the *A* site. We may examine these arrangements and their relation to the *A*-cation behavior in a straightforward fashion using the graphs shown in Figure 4b. The vertices of the hexagon are *T* sites, and *T* sites occupied by Al are marked by black or white circles, depending on whether they occur in the upper (black) or lower (white) hexagonal ring of tetrahedra. It is immediately apparent that there are five distinct arrangements (Fig. 4b). The *A* cation will tend to positionally disorder such as to bond more strongly to the O(5) and O(7) or O(6) and O(7) anions of the tetrahedra that contain Al in order to compensate for the reduced bond-valence incident at these anions from the *T* (= Al) cation. In arrangements (3) and (5), $^{T(1)}$Al is asymmetrically arranged around the *A* cavity, and occupancy of the *A*(2) position by Na ensures strong bonding with the O(5), O(6) and O(7) anions of the *T*(1) = Al tetrahedra (Fig. 4b). The situation is less clear for arrangements (1), (2) and (4); the optimum position for the *A* cation would seem to be at the *A*2/*m* site, but this site cannot be occupied (see above). To resolve this situation, one must consider the effect of adjacent *A* cavities. This effect is shown in Figure 4c for some of the possible combinations of the arrangements of Figure 4b. As is apparent from Figure 4a, the O(7) anion always bonds to an *A*(2) cation, but only half of the O(5) and O(6) anions bond to an *A*(2) cation. Hence the *A* cation will adopt the specific combination of *A*(2) sites in adjacent cavities of the chain such that the number of bonds from $^{A(2)}$Na to O(5) and O(6) involved in Al–O–Si linkages is maximized. This behavior may easily be put on a quantitative basis by counting the fraction of Al–O(5,6)–Si linkages in which O(5) or O(6) bonds to the *A*(2) cation. Consider the arrangements in Figure 4b repeated by translational symmetry; the fractions of Al–O(5,6)–Si linkages adjacent to an *A*(2) cation are 0.50, 0.50, 1.0, 0.50 and 0.75 for arrangements (1) to (5), respectively, and combination of the different arrangements (3) and (5) (Fig. 4b) will be favored over arrangements (1), (2) and (4), as in the former, all local bond-valence requirements of the anions are satisfied primarily by order of nearest-neighbor cations, whereas in the latter, the bond-valence requirements of the anions need significant transfer of bond-valence from NNNN (next-next-nearest neighbor) cations *via* relaxation of intervening bonds.

There is one more aspect of pattern of *A*(2) order in adjacent chains that needs to be considered, and this is most easily seen by comparing arrangement (1′) with arrangement (2′) in Figure 4c. In these two arrangements, the pattern of order *within* each double-chain of tetrahedra is the same, and the same fraction (0.50) of O(5) and O(6) anions involved in Al–O–Si linkages bonds to Na at *A*(2). However, in arrangement (1′), all tetrahedra occupied by Al have either O(5) or O(6) bonded to $^{A(2)}$Na, whereas in arrangement (2′), half the tetrahedra occupied by Al have both O(5) and O(6) bonded to $^{A(2)}$Na, and half the tetrahedra occupied by Al have both O(5) and O(6) adjacent to $^{A(2)}\square$. Arrangement (1′) can adjust much more easily than arrangement (2′) (Fig. 4c), *via* bond-length relaxation, such that the bond-valence requirements are satisfied at the O(5) and O(6) anions adjacent to $^{A(2)}\square$. Thus arrangements such as (2′) (Fig. 4c), which result in *T*(1) = Al tetrahedra in which neither O(5) nor O(6) bond to $^{A(2)}$Na, will be even less favored than arrangements such as (1′) (Fig. 4c).

The behavior of the *A*(*m*) site is quite different from that of the *A*(2) site with regard to local order. The *A*(2) site lies to one side of the *A* cavity, and only contributes bond-valence to half of the *A*-cavity in which it occurs. Thus in Figure 4a, it is evident that an amphibole with the *A* cavity completely occupied by Na at *A*(2) will have *two* local configurations, one associated with an occupied *A*(2) site and the other associated with an unoccupied *A*(2) site. The *A*(*m*) site also lies to one side of the *A* cavity (Fig. 5a), but that side of the *A* cavity is adjacent to another *A* cavity (Fig. 5b). This means that in an ordered chain with a full *A* site, there is only *one* local configuration associated with an occupied *A*(*m*) site in one *A* cavity and an unoccupied *A*(*m*) site in the adjacent *A* cavity. The possibility for local order of *A*(*m*) cations comes from the occupancy of adjacent *A*(*m*) sites in adjacent cavities; this may produce the two local arrangements shown in Figure 5b. Note that this results in an important difference between the environment of the O(7) anion in calcic *versus* alkali amphiboles. In calcic amphiboles, O(7) can link to only one *A*(2) cation, whereas in alkali amphiboles, O(7) can link to two *A*(*m*) cations [coupled with another local configuration in which the O(7) anion does not link to an *A*(*m*) cation]. Hence all local configurations in calcic amphiboles with a fully occupied *A* site must involve an *A*(2) cation bonded to O(7), whereas in alkali amphiboles with a fully occupied *A* site, some local configurations do not necessarily involve an *A*(*m*) cation bonded to O(7). Note that this argument applies to ^{A}Na only; ^{A}K always orders at the *A*(*m*) site [a more extensive discussion of short-range order involving ^{A}Na and ^{A}K is given in Hawthorne *et al.* (1996a)].

In order to simplify the presentation of the bond-valences associated with the cations at the *A* site(s), the bond-valence tables presented here show only one entry column for the *A* site. For occupancy of the *A*(2) site, there are six relatively strong (≥0.10 *vu*) bonds, two to O(5), two to O(6) and two to O(7). For occupancy of the *A*(*m*) site, there are eight relatively strong bonds, four to O(5), two to O(6) and two to O(7). These two situations are accommodated in the bond-valence tables by always assigning a multiplicity of ×2 to the *A*–O(5) bond. Where *A*(2) is occupied, there are two strong *A*(2)–O(5) bonds, as indicated in the table. Where *A*(*m*) is occupied, there are four weaker *A*(*m*)–O(5) bonds; thus if the *A*–O(5) bond-valence is doubled and its multiplicity is halved (to ×2), the bond-valence sum at *A* remains correct. For full details of the SRO associated

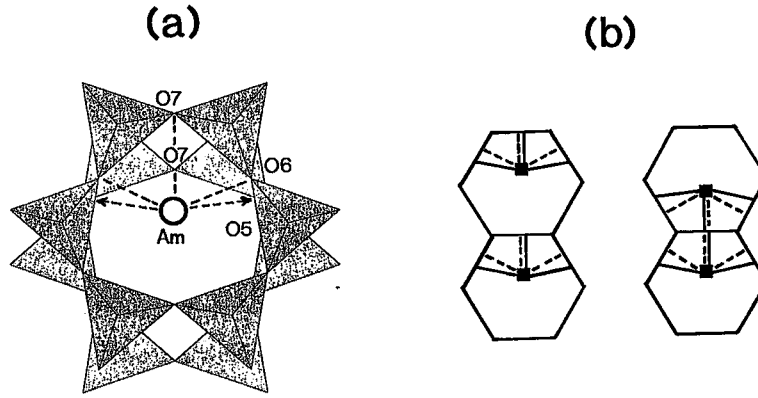

FIG. 5. Details of short-range order involving the $A(m)$ site in pargasite: (a) the A cavity, surrounded by two hexagonal rings of $T(1)$ and $T(2)$ tetrahedra, with the $A(m)$ site indicated by a circle; (b) graphs of two possible arrangements of short-range order in adjacent A-cavities.

with occupancy of the $A(2)$ and $A(m)$ sites, see Hawthorne *et al.* (1996a).

A FUNDAMENTAL BUILDING BLOCK (FBB) FOR PATTERNS OF SRO

When dealing with SRO, it is important to define the unit of structure with which one is working. Figure 6 shows the specific unit used here, a trimer of $M(1)$, $M(2)$ and $M(3)$ octahedra linked in the a direction to a dimer of $T(1)$ and $T(2)$ tetrahedra, together with its related $M(4)$ and A sites; the bond-valence tables used here refer specifically to this unit. Bond-valence contributions from adjacent units are also of importance, and are specifically identified in the following tables. It is important to identify this unit, as different experimental methods are sensitive to different types of local configuration, and these cannot easily be analyzed if the unit is not explicitly identified.

CALCIC AMPHIBOLES

Pargasite

Pargasite, $NaCa_2(Mg_4Al)(Si_6Al_2)O_{22}(OH)_2$, has Si and Al as T-group cations, and Mg and Al as C-group cations; combined with the presence of an A-site cation, this stoichiometry gives a large number of possible arrangements. In pargasite, $^{[4]}$Al is usually completely ordered at the $T(1)$ site (Oberti *et al.* 1995b) and ^{A}Na is ordered at the $A(2)$ site (Hawthorne *et al.* 1996a); $^{[6]}$Al is partly disordered between $M(2)$ and $M(3)$ in Fe-poor pargasite (Oberti *et al.* 1995a), and may be completely disordered between $M(2)$ and $M(3)$ in synthetic end-member pargasite (Welch *et al.* 1994, Della Ventura *et al.* 1996c, d). These are patterns of long-range order. One also expects $^{A(2)}$Na to be *locally* associated with $^{T(1)}$Al in order to compensate for the reduced bond-valence at the O(5), O(6) and O(7) anions incident from the $T(1)$ cation. Of the possible local arrangements, Table 3 shows those which most closely satisfy the

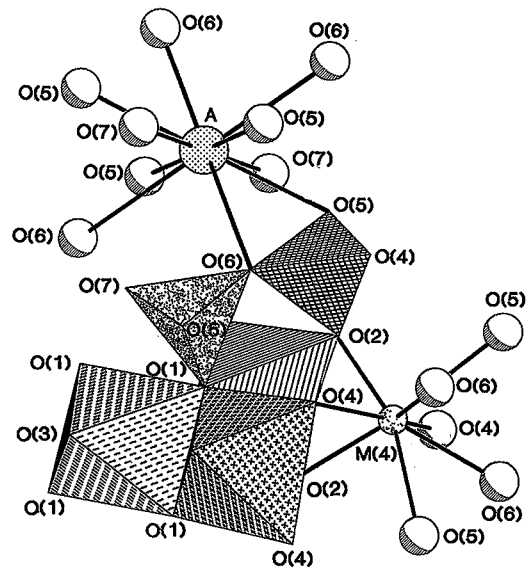

FIG. 6. The FBB used in the consideration of bond-valence aspects of the amphibole structure.

valence-sum rule. Arrangement (1) has $A(2)$ = Na, $M(2)$ = Al, $T(1)$ = Al (Table 4), and the bond-valence sums around the anions are close to their ideal values (Table 3). Aluminum at $T(1)$ gives reduced bond-valence to O(1), O(5), O(6) and O(7), and this is compensated by bonds to these anions from Al at

TABLE 3. BOND-VALENCE TABLES FOR PROPOSED SHORT-RANGE ARRANGEMENTS IN CALCIC AMPHIBOLES

Pargasite: arrangement (1)

	M(1)	M(2)	M(3)	M(4)	A	T(1)	T(2)	Σ
O(1)	0.41$^{\times2}\downarrow$	0.52$^{\times2}\downarrow$	0.33$^{\times1}\downarrow$			0.75		2.01
O(2)	0.25$^{\times2}\downarrow$	0.46$^{\times2}\downarrow$		0.28$^{\times2}\downarrow$			1.01	2.00
O(3)	0.34$^{\times2}\downarrow\rightarrow$		0.33$^{\times2}\downarrow$					1.00
O(4)		0.52$^{\times2}\downarrow$		0.35$^{\times2}\downarrow$			1.08	1.95
O(5)				0.14$^{\times2}\downarrow$	0.15$^{\times2}\downarrow$	0.75	0.96	2.00
O(6)				0.23$^{\times2}\downarrow$	0.10$^{\times2}\downarrow$	0.75	0.95	2.03
O(7)					0.25$^{\times2}\downarrow$	0.75/1.00		2.00
Σ	2.00	3.00	1.98	2.00	1.00	3.00	4.00	

Pargasite: arrangement (2)

	M(1)	M(2)	M(3)	M(4)	A	T(1)*	T(2)	Σ
O(1)	0.33$^{\times2}\downarrow$	0.27$^{\times2}\downarrow$	0.33$^{\times1}\downarrow$			1.10		2.03
O(2)	0.33$^{\times2}\downarrow$	0.33$^{\times2}\downarrow$		0.30$^{\times2}\downarrow$			1.05	2.01
O(3)	0.34$^{\times2}\downarrow\rightarrow$		0.33$^{\times2}\downarrow$					1.00
O(4)		0.40$^{\times2}\downarrow$		0.36$^{\times2}\downarrow$			1.10	1.86
O(5)				0.13$^{\times2}\downarrow$	–	1.00	0.95	2.08
O(6)				0.21$^{\times2}\downarrow$	–	0.96	0.90	2.07
O(7)					–/0.21$^{\times2}\downarrow$	0.94$^{\times2}\rightarrow$		2.09
Σ	2.00	2.00	1.98	2.00	–	4.00	4.00	

Pargasite: arrangement (3)

	M(1)	M(2)	M(3)	M(4)	A	T(1)*	T(2)	Σ
O(1)	0.40$^{\times2}\downarrow$	0.32$^{\times2}\downarrow$	0.50$^{\times1}\downarrow$			0.75		1.97
O(2)	0.36$^{\times2}\downarrow$	0.30$^{\times2}\downarrow$		0.30$^{\times2}\downarrow$			1.00	1.96
O(3)	0.24$^{\times2}\downarrow\rightarrow$		0.50$^{\times2}\downarrow$					0.98
O(4)		0.38$^{\times2}\downarrow$		0.35$^{\times2}\downarrow$			1.10	1.83
O(5)				0.14$^{\times2}\downarrow$	0.15$^{\times2}\downarrow$	0.75	0.96	2.00
O(6)				0.21$^{\times2}\downarrow$	0.10$^{\times2}\downarrow$	0.75	0.94	2.00
O(7)					0.25$^{\times2}\downarrow$	0.75/1.00		2.00
Σ	2.00	2.00	3.00	2.00	1.00	3.00	4.00	

Pargasite: arrangement (4)

	M(1)	M(2)	M(3)	M(4)	A	T(1)*	T(2)	Σ
O(1)	0.33$^{\times2}\downarrow$	0.20$^{\times2}\downarrow$	0.50$^{\times1}\downarrow$			1.00		2.03
O(2)	0.33$^{\times2}\downarrow$	0.40$^{\times2}\downarrow$		0.28$^{\times2}\downarrow$			1.00	2.01
O(3)	0.34$^{\times2}\downarrow\rightarrow$		0.50$^{\times2}\downarrow$					1.18
O(4)		0.40$^{\times2}\downarrow$		0.45$^{\times2}\downarrow$			1.10	1.95
O(5)				0.14$^{\times2}\downarrow$	–	1.00	0.95	2.09
O(6)				0.13$^{\times2}\downarrow$	–	1.00	0.95	2.08
O(7)					–	1.00/0.75		1.75
Σ	2.00	2.00	3.00	2.00	–	4.00	4.00	

Edenite: arrangement (1)

	M(1)	M(2)	M(3)	M(4)	A	T(1)*	T(2)	Σ
O(1)	0.37$^{\times2}\downarrow$	0.32$^{\times2}\downarrow$	0.33$^{\times1}\downarrow$			0.85		1.87
O(2)	0.30$^{\times2}\downarrow$	0.30$^{\times2}\downarrow$		0.28$^{\times2}\downarrow$			1.07	1.95
O(3)	0.33$^{\times2}\downarrow\rightarrow$		0.34$^{\times2}\downarrow$					1.00
O(4)		0.38$^{\times2}\downarrow$		0.35$^{\times2}\downarrow$			1.10	1.83
O(5)				0.14$^{\times2}\downarrow$	0.17$^{\times2}\downarrow$	0.70	0.92	1.93
O(6)				0.23$^{\times2}\downarrow$	0.12$^{\times2}\downarrow$	0.70	0.91	1.96
O(7)					0.21$^{\times2}\downarrow$	0.75/1.00		1.96
Σ	2.00	2.00	2.00	2.00	1.00	3.00	4.00	

TABLE 3. continued

Edenite: arrangement (3)

	M(1)	M(2)	M(3)	M(4)	A	T(1)	T(2)	Σ
O(1)	0.34$^{\times2}\downarrow$	0.30$^{\times2}\downarrow$	0.33$^{\times1}\downarrow$			1.10		2.07
O(2)	0.33$^{\times2}\downarrow$	0.30$^{\times2}\downarrow$		0.30$^{\times2}\downarrow$			1.16	2.09
O(3)	0.33$^{\times2}\downarrow\rightarrow$		0.34$^{\times2}\downarrow$					1.00
O(4)		0.40$^{\times2}\downarrow$		0.36$^{\times2}\downarrow$			1.15	1.91
O(5)				0.13$^{\times2}\downarrow$	0.15$^{\times2}\downarrow$	1.00	0.87	2.15
O(6)				0.21$^{\times2}\downarrow$	0.10$^{\times2}\downarrow$	1.00	0.82	2.13
O(7)					0.25$^{\times2}\downarrow$	0.90$^{\times2}\rightarrow$		2.05
Σ	2.00	2.00	2.00	2.00	1.00	4.00	4.00	

Sadanagaite: arrangement (2)

	M(1)	M(2)	M(3)	M(4)	A	T(1)	T(2)	Σ
O(1)	0.27$^{\times2}\downarrow$	0.40$^{\times2}\downarrow$	0.33$^{\times1}\downarrow$			1.00		2.00
O(2)	0.40$^{\times2}\downarrow$	0.48$^{\times2}\downarrow$		0.28$^{\times2}\downarrow$			0.74	1.90
O(3)	0.33$^{\times2}\downarrow\rightarrow$		0.34$^{\times2}\downarrow$					1.00
O(4)		0.62$^{\times2}\downarrow$		0.38$^{\times2}\downarrow$			0.81	1.81
O(5)				0.14$^{\times2}\downarrow$	–	1.00	0.75	1.89
O(6)				0.20$^{\times2}\downarrow$	–	1.00	0.70	1.90
O(7)					–	1.00$^{\times2}\rightarrow$		2.00
Σ	2.00	3.00	2.00	2.00	–	4.00	3.00	

Tschermakite: arrangement (1)

	M(1)	M(2)	M(3)	M(4)	A	T(1)*	T(2)	Σ
O(1)	0.36$^{\times2}\downarrow$	0.52$^{\times2}\downarrow$	0.33$^{\times1}\downarrow$			0.75		1.96
O(2)	0.31$^{\times2}\downarrow$	0.44$^{\times2}\downarrow$		0.28$^{\times2}\downarrow$			0.93	1.96
O(3)	0.33$^{\times2}\downarrow\rightarrow$		0.34$^{\times2}\downarrow$					1.00
O(4)		0.54$^{\times2}\downarrow$		0.30$^{\times2}\downarrow$			1.00	1.84
O(5)				0.19$^{\times2}\downarrow$	–	0.70	1.05	1.94
O(6)				0.23$^{\times2}\downarrow$	–	0.70	1.02	1.95
O(7)					–	0.85/1.10		1.95
Σ	2.00	3.00	2.00	2.00	–	3.00	4.00	

Tschermakite: arrangement (2)

	M(1)	M(2)	M(3)	M(4)	A	T(1)*	T(2)	Σ
O(1)	0.33$^{\times2}\downarrow$	0.42$^{\times2}\downarrow$	0.33$^{\times1}\downarrow$			1.00		2.08
O(2)	0.33$^{\times2}\downarrow$	0.46$^{\times2}\downarrow$		0.28$^{\times2}\downarrow$			1.00	2.07
O(3)	0.34$^{\times2}\downarrow\rightarrow$		0.34$^{\times2}\downarrow$					1.02
O(4)		0.62$^{\times2}\downarrow$		0.35$^{\times2}\downarrow$			1.00	1.97
O(5)				0.14$^{\times2}\downarrow$	–	1.00	1.00	2.14
O(6)				0.23$^{\times2}\downarrow$	–	0.90	1.00	2.13
O(7)					–	1.10/0.85		2.00
Σ	2.00	3.00	2.00	2.00	–	4.00	4.00	

* O(7) is bonded to two $T(1)$ cations. In some local arrangements (and always in long-range arrangements), these two $T(1)$ cations are identical and the bond-valence sum at O(7) involves a ×2→ symbol. In other local arrangements, the two $T(1)$ cations are different, and the bond-valence sum involves two different contributions from the $T(1)$ site [*e.g.*, 0.75/1.00 for pargasite arrangement (1)]. However, the bond-valence sum at the $T(1)$ site for a specific local arrangement involves only one of the two bond-valence entries for the $T(1)$–O(7) bond. In these tables, the first of the two entries [*e.g.* 0.75 for pargasite arrangement (1)] is the value that contributes to the sum at the $T(1)$ site.

TABLE 4. PROPOSED SHORT-RANGE ARRANGEMENTS IN CALCIC AMPHIBOLES

Amphibole	*M*(1)	*M*(2)	*M*(3)	*M*(4)	*A*(*m*)	*A*(2)	*T*(1)	*T*(2)	Arrangement
Tremolite	Mg	Mg	Mg	Ca	–	–	Si	Si	Tremolite
Pargasite	Mg	Al	Mg	Ca	–	Na	Al	Si	Pargasite (1)
	Mg	Mg	Mg	Ca	–	–	Si	Si	Pargasite (2)
	Mg	Mg	Al	Ca	–	Na	Al	Si	Pargasite (3)
	Mg	Mg	Al	Ca	–	–	Si	Si	Pargasite (4)
Edenite	Mg	Mg	Mg	Ca	–	Na	Al	Si	Edenite (1)
	Mg	Mg	Mg	Ca	–	–	Si	Si	Edenite (2) [≡Pargasite (2)]
	Mg	Mg	Mg	Ca	–	Na	Si	Si	Edenite (3)
Sadanagaite	Mg	Al	Mg	Ca	–	Na	Al	Si	Sadanagaite (1) [≡Pargasite (1)]
	Mg	Al	Mg	Ca	–	–	Si	Al	Sadanagaite (2)
Tschermakite	Mg	Al	Mg	Ca	–	–	Al	Si	Tschermakite (1)
	Mg	Al	Mg	Ca	–	–	Si	Si	Tschermakite (2)
Hornblende	Mg	Al	Mg	Ca	–	–	Al	Si	Hornblende (1) [≡Tschermakite (1)]
	Mg	Mg	Mg	Ca	–	–	Si	Si	Hornblende (2) [≡Tremolite]

M(2) and Na at *A*(2). Note that the short-range coupling between these site-occupancies can extend throughout the structure for ideally ordered pargasite, with *M*(2) = Al_1Mg_1 and *T*(1) = Si_2Al_2. Each Si–Al pair of *T*(1) tetrahedra link to an Mg–Al pair of *M*(2) octahedra in the strip of octahedra (Fig. 7); this linkage occurs on *both* sides of the strip of octahedra, so that each *M*(2) = Al octahedron is associated with *two* *T*(1) = Al tetrahedra such that the local order is commensurate with the chemical composition of the crystal, unlike the corresponding situation in edenite. Where *T*(1) = Si, *A*(2) = □ and *M*(2) = Mg, the local bond-valence arrangement is that of tremolite, except for the fact that there is an additional bond to O(7) from an *A*(2) cation in an adjacent configuration [arrangement (2)]. Thus pargasite with *M*(2) = Al_1Mg_1 and *T*(1) = Si_2Al_2 has two SRO arrangements [(1) and (2)] that occur in equal amounts, and sum to the chemical composition of the bulk crystal. An arrangement with *M*(1) = *M*(2) = *M*(3) = Mg, *A* = Na, *T*(1) = Al also is feasible from a bond-valence viewpoint [≡ arrangement (1) for edenite], but probably does not occur, as it also forces the arrangement *M*(1) = *M*(3) = Mg, *M*(2) = Al, *A* = □, *T*(1) = T(2) = Si, which has major deviations from the valence-sum rule.

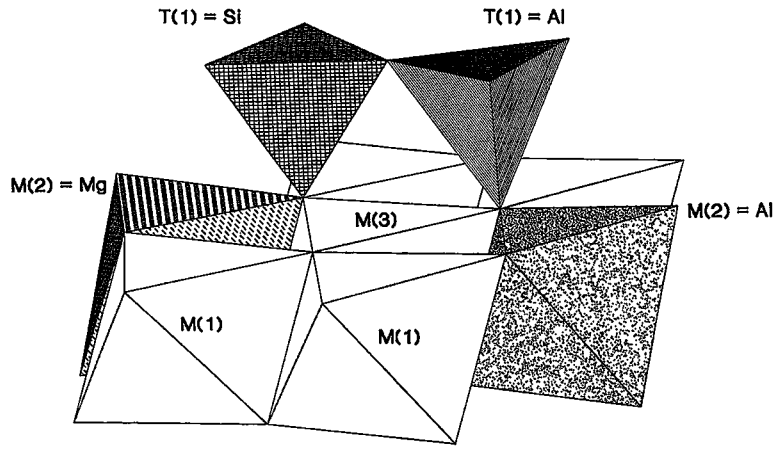

FIG. 7. Possible coupling between Al and Si occupancy of *T*(1) and Al and Mg occupancy of *M*(2) in pargasite such that $^{T(1)}$Al links to O(1) bonded to $^{M(2)}$Al and $^{T(1)}$Si links to O(1) bonded to $^{M(2)}$Mg.

The above arrangements hold for pargasite with large divalent cations [*e.g.*, M^{2+} = (Mg≈Fe^{2+})] (Oberti *et al.* 1995a) or Co^{2+} (Della Ventura *et al.* 1996c) at the *M*(1) and *M*(3) sites. In Fe-poor pargasite and synthetic pargasite, *M*(3) = (Mg,Al) and *M*(2) = (Mg>Al), and hence there must also be local configurations involving *M*(3) = Al. The optimum arrangement is shown in Table 3, arrangement (3). The strong *M*(3)–O(1) bond partly compensates for the decrease in *T*(1)–O(1) bond-valence, together with cooperative shortening of the *M*(1)–O(1) bond and lengthening of the *M*(1)–O(3) bond. Thus arrangement (3) conforms as well to the valence-sum rule as arrangement (1). However, arrangement (3) must also be associated with arrangement (4) (Table 3), in which *M*(2) = Mg, *M*(3) = Al, *T*(1) = Si. This arrangement resembles that in tremolite, except that the *M*(3) cation is replaced by Al. Thus, although the arrangement conforms to the valence-sum rule reasonably well, it requires dispersion of some bond-valence to adjacent arrangements.

Edenite

Edenite, $NaCa_2Mg_5(Si_7Al)O_{22}(OH)_2$, has both Si and Al as *T*-group cations, and hence there must be different local configurations associated with occupancy of a specific *T* site by Si *or* by Al. In general, where $^{[4]}Al \leq 2.0$ *apfu*, Al is ordered at the *T*(1) site, and thus we need to consider two configurations, one in which Al occurs at the *T*(1) site, and the other in which Si occurs at the *T*(1) site. Where *T*(1) = Al, $^{A(2)}Na$ is locally associated with $^{T(1)}Al$ in order to compensate for the reduced bond-valence incident at the O(5), O(6) and O(7) anions, and the arrangement is edenite arrangement (1) (Table 3). Where *T*(1) is occupied by Si, the local bond-valence arrangement is that of pargasite (2). The *A*(2) site associated with *T*(1) = Si is unoccupied; ^{A}Na occupies the *A*(2) site on the other side of the *A* cavity where *T*(1) = Al. Examination of the amphibole structure shows that where ^{A}Na occupies an *A*(2) site on one site of the *A* cavity, it must be associated not only with *T*(1) = Al, but also with *T*(1) = Si. Hence one quarter of the local arrangements in edenite are equivalent to a tremolite arrangement with an additional Na, the edenite arrangement (3) (Table 3). This may perhaps be accommodated by relaxation of bond lengths in this arrangement and in the adjacent pargasite (2) and edenite(1) arrangements, but it also may account for the fact that compositions near end-member edenite are rare or absent in Nature.

Sadanagaite

The structure of sadanagaite, $NaCa_2(Mg_3Al_2)(Si_5Al_3)O_{22}(OH)_2$, has not been refined, and hence the details of long-range order are not established. However, the following scheme seems reasonable: *M*(1) = Mg_2, *M*(2) = Al_2, *M*(3) = Mg, although $^{M(3)}Al$ cannot be discounted, and *T*(1) = Si_2Al_2, *T*(2) = Si_3Al_1, as indicated for the Si_5Al_3 chain with no Al–O–Al linkages in Figure 3c. Thus the principal local arrangements will involve $^{[4]}Al$ and Si at *T*(1) and *T*(2), and Na and □ (vacancy) at the *A* site. As the details of the ^{A}Na arrangement are not known, there are additional possibilities in the consideration of local bond-valences. Arrangement (1) has *T*(1) = Al, *T*(2) = Si, *M*(2) = Al, *A*(2) = Na, and is the pargasite arrangement (1). Arrangement (2) has *T*(1) = Si, *T*(2) = Al and *M*(2) = Al; the situation with regard to ^{A}Na is not clear, although if half the configurations are arrangement (1) (the pargasite arrangement) and involve *A*(2) = Na, then the other half of the configurations [sadanagaite arrangement (2)] *must* involve *A*(2) = □. As shown in Table 3, this produces reasonable bond-valence sums around all anions. Thus sadanagaite is expected to be a 50:50 mixture of these two local arrangements (Table 4).

Tschermakite

Tschermakite, $□Ca_2(Mg_3Al)(Si_6Al_2)O_{22}(OH)_2$, has *M*(1) = Mg_2, *M*(2) = Al_2, *M*(3) = Mg_1, *T*(1) = Si_2Al_2 and *T*(2) = Si_4, and hence the only local order involves Al and Si at the *T*(1) site. Arrangement (1) (Table 3) involves *T*(1) = Al, and arrangement (2) involves *T*(1) = Si. Agreement with the valence-sum rule is good for arrangement (1) and reasonable for arrangement (2). However, arrangement (1) involves a slight deficiency of bond-valence at each anion, whereas arrangement (2) involves an excess at some of the anions, suggesting that there should be some relaxation in bond lengths between the two arrangements, which occur in a 50:50 ratio (Table 4).

Hornblende

Hornblende, $□Ca_2(Mg_4Al)(Si_7Al)O_{22}(OH)_2$, is intermediate in composition between tremolite and tschermakite, and has *M*(1) = Mg_2, *M*(2) = Al_1Mg_1, *M*(3) = Mg_1, *T*(1) = Si_3Al_1 and *T*(2) = Si_4. There are two possible optimum arrangements (Table 4): arrangement (1) is identical to arrangement (1) in tschermakite, and arrangement (2) is identical to the arrangement in tremolite. Thus hornblende avoids the less favorable arrangement (2) of tschermakite, possibly accounting for the fact that synthetic amphiboles can be grown along the tremolite–tschermakite join only as far as the hornblende composition (Jenkins 1994), and for the absence of natural amphiboles near tschermakite end-member composition.

Alkali Amphiboles

Eckermannite

Eckermannite, $NaNa_2(Mg_4Al)Si_8O_{22}(OH)_2$, has *A*(*m*) = Na (Hawthorne *et al.* 1996a) and *M*(2) = Al_1Mg_1

TABLE 5. BOND-VALENCE TABLES FOR PROPOSED SHORT-RANGE ARRANGEMENTS IN ALKALI AMPHIBOLES

Eckermannite: arrangement (1)

	M(1)	*M*(2)	*M*(3)	*M*(4)	*A*	*T*(1)	*T*(2)	Σ
O(1)	$0.33^{\times 2}\downarrow$	$0.24^{\times 2}\downarrow$	$0.33^{\times 1}\downarrow$			1.12		2.02
O(2)	$0.34^{\times 2}\downarrow$	$0.34^{\times 2}\downarrow$		$0.16^{\times 2}\downarrow$			1.10	1.95
O(3)	$0.33^{\times 2}\downarrow\rightarrow$		$0.34^{\times 2}\downarrow$					1.00
O(4)		$0.42^{\times 2}\downarrow$		$0.20^{\times 2}\downarrow$			1.23	1.85
O(5)				$0.04^{\times 2}\downarrow$	$0.10^{\times 2}\downarrow$	1.02	0.85	2.01
O(6)				$0.10^{\times 2}\downarrow$	$0.06^{\times 2}\downarrow$	1.03	0.82	2.01
O(7)					$0.34^{\times 2}\downarrow$	$0.83^{\times 2}\rightarrow$		2.00
Σ	2.00	2.00	2.00	2.00	1.00	4.00	4.00	

Nyböite: arrangement (1)

	M(1)	*M*(2)	*M*(3)	*M*(4)	*A*	*T*(1)	*T*(2)	Σ
O(1)	$0.34^{\times 2}\downarrow$	$0.40^{\times 2}\downarrow$	$0.33^{\times 1}\downarrow$			0.90		1.98
O(2)	$0.33^{\times 2}\downarrow$	$0.50^{\times 2}\downarrow$		$0.14^{\times 2}\downarrow$			1.00	1.97
O(3)	$0.33^{\times 2}\downarrow\rightarrow$		$0.34^{\times 2}\downarrow$					1.00
O(4)		$0.60^{\times 2}\downarrow$		$0.17^{\times 2}\downarrow$			1.08	1.85
O(5)				$0.06^{\times 2}\downarrow$	$0.17^{\times 2}\downarrow$	0.80	0.98	2.01
O(6)				$0.13^{\times 2}\downarrow$	$0.12^{\times 2}\downarrow$	0.80	0.94	1.99
O(7)					$0.21^{\times 2}\downarrow$	0.60/1.00		1.81
Σ	2.00	3.00	2.00	1.00	1.00	3.10	4.00	

(Hawthorne *et al.* 1993b), and hence the possibilities of local order involve Al and Mg at $M(2)$, and Na and □ at $A(m)$. Arrangement (1) involves $M(2)$ = Mg, $A(m)$ = Na (Tables 5, 6) and shows very good agreement with the valence-sum rule. Arrangement (2) must involve $M(2)$ = Al, $A(m)$ = □ (Table 6) and is the glaucophane arrangement.

Nyböite

Nyböite, $NaNa_2(Mg_3Al_2)(Si_7Al)O_{22}(OH)_2$, has $M(2)$ = Al, $A(m)$ = Na (Hawthorne *et al.* 1996a) and $T(1) = Si_3Al_1$, and hence the possibilities for local order involve Si and Al at $T(1)$, and Na and □ at $A(m)$. Arrangement (1) involves Na at $A(m)$ and Al at $T(1)$ and shows very good agreement with the valence-sum rule (Table 5). Arrangement (2) has Si at $T(1)$ and □ at $A(m)$, and is the glaucophane arrangement (Table 6). Other arrangements, such as Al at $T(1)$ and □ at $A(m)$, and Si at $T(1)$ and Na at $A(m)$, depart considerably from the valence-sum rule, and hence are much less likely to occur.

Sodic–Calcic Amphiboles

The sodic–calcic amphiboles are intermediate in composition between the calcic and the alkali amphiboles, and accordingly, their optimum patterns of order are usually combinations of those observed in calcic and alkali amphiboles. These are summarized in Table 7. Winchite, $\square CaNa(Mg_4Al)Si_8O_{22}(OH)_2$, has $M(4) = Na_1Ca_1$ and $M(2) = Al_1Mg_1$. The optimum local arrangements involve $M(2)$ = Al, $M(4)$ = Na and $M(2)$ = Mg, $M(4)$ = Ca. Thus winchite has the local arrangements of glaucophane and tremolite (Table 7). Barroisite, $\square CaNa(Mg_3Al_2(Si_7Al)O_{22}(OH)_2$, has $M(4) = Na_1Ca_1$ and $T(1) = Si_3Al_1$, and the optimum local arrangements involve $M(4)$ = Na, $T(1)$ = Si (glaucophane), $M(4)$ = Ca, $T(1)$ = Al [tschermakite (1)], and $M(4)$ = Ca, $T(1)$ = Si [tschermakite (2)].

Richterite, $NaCaNa(Mg_5)Si_8O_{22}(OH)_2$, has $M(4) = Na_1Ca_1$, and local order must involve coupling between $M(4)$ and the A site. Details of the A-site arrangement in richterite are not known, but ^{A}Na occupies the $A(1)$ site in fluor-richterite (Cameron *et al.* 1983, Hawthorne *et al.* 1996a), closer to the $A(2)$ site than the $A(m)$ site, and thus for richterite, ^{A}Na is

TABLE 7. PROPOSED SHORT-RANGE ARRANGEMENTS IN SODIC-CALCIC AMPHIBOLES

Amphibole	*M*(1)	*M*(2)	*M*(3)	*M*(4)	*A*(*m*)	*A*(2)	*T*(1)	*T*(2)	Arrangement
Winchite	Mg	Mg	Mg	Ca	–	–	Si	Si	Winchite (1) [= Tremolite]
"	Mg	Al	Mg	Na	–	–	Si	Si	Winchite (2) [= Glaucophane]
Barroisite	Mg	Al	Mg	Ca	–	–	Al	Si	Barroisite (1) [= Tschermakite (1)]
"	Mg	Al	Mg	Ca	–	–	Si	Si	Barroisite (2) [= Tschermakite (2)]
"	Mg	Al	Mg	Na	–	–	Si	Si	Barroisite (3) [= Glaucophane]
Richterite	Mg	Mg	Mg	Ca	–	–	Si	Si	Richterite (1) [= Pargasite (2)]
"	Mg	Mg	Mg	Na	–	Na	Si	Si	Richterite (2) [= Eckermannite (1)]
Taramite	Mg	Al	Mg	Ca	–	Na	Al	Si	Taramite (1) [= Pargasite (1)]
"	Mg	Al	Mg	Na	–	–	Si	Si	Taramite (2) [= Barroisite (3)]
Katophorite	Mg	Mg	Mg	Ca	–	Na	Al	Si	Katophorite (1) [= Edenite (1)]
"	Mg	Mg	Mg	Ca	–	Na	Si	Si	Katophorite (2)
"	Mg	Al	Mg	Na	–	–	Si	Si	Katophorite (3) [= Barroisite (3)]

TABLE 6. PROPOSED SHORT-RANGE ARRANGEMENTS IN ALKALI AMPHIBOLES

Amphibole	*M*(1)	*M*(2)	*M*(3)	*M*(4)	*A*(*m*)	*A*(2)	*T*(1)	*T*(2)	Arrangement
Glaucophane	Mg	Al	Mg	Na	–	–	Si	Si	Glaucophane
Eckermannite	Mg	Mg	Mg	Na	Na	–	Si	Si	Eckermannite (1)
"	Mg	Al	Mg	Na	–	–	Si	Si	Eckermannite (2) [= Glaucophane]
Nyböite	Mg	Al	Mg	Na	Na	–	Al	Si	Nyböite (1)
"	Mg	Al	Mg	Na	–	–	Si	Si	Nyböite (2) [= Glaucophane]
Leakeite	Mg	Al	Li	Na	Na	–	Si	Si	Leakeite
Ungarettiite	Mn^{3+}	Mn^{2+}	Mn^{3+}	Na	Na	–	Si	Si	Ungarettiite

assumed to occupy the $A(2)$ site. There are two distinct arrangements, pargasite (2) and eckermannite (1). Taramite, $NaCaNa(Mg_3Al_2)(Si_6Al_2)O_{22}(OH)_2$, has $M(4) = Na_1Ca_1$ and $T(1) = Si_2Al_2$. In addition, Hawthorne *et al.* (1996a) have shown that ^{A}Na is ordered at the $A(2)$ site in taramite and is locally associated with Ca at the $M(4)$ site. Thus the optimum local arrangements involve $M(4)$ = Ca, $T(1)$ = Al, $A(2)$ = Na [pargasite (1)] and $M(4)$ = Na, $T(1)$ = Si, $A(2) = \square$ [which is the glaucophane arrangement with the addition of a single $A(2)$–O(7) bond (Table 8) from an adjacent pargasite (1) arrangement]. Other schemes of local order are possible, but are less likely on bond-valence grounds. For example, a combination of nyböite (1) and tschermakite(2) arrangements is possible, but in nyböite, ^{A}Na occupies the $A(m)$ site, whereas in taramite, the $A(m)$ site is vacant and the $A(2)$ site is occupied; hence local arrangements of nyböite with an unfavorable A-site occupancy are unlikely. Katophorite, $NaCaNa(Mg_4Al)(Si_7Al)O_{22}(OH)_2$, has $M(4) = Na_1Ca_1$, $M(2) = Al_1Mg_1$ and $T(1) = Si_3Al_1$ and ^{A}Na completely ordered at $A(2)$ (Hawthorne *et al.* 1996a). In principle, a large number of patterns of order are possible. However, Hawthorne *et al.* (1996a) have shown that Ca at $M(4)$ is locally associated with Na at $A(2)$, which restricts somewhat the possible local arrangements. The optimum arrangements with regard to the valence-matching principle are shown in Table 7. Katophorite arrangement (2) is shown in Table 8; it may be envisaged as a tremolite arrangement with the addition of Na at the A site, and hence will need to disperse bond-valence to the surrounding arrangements. Other possible arrangements show much more deviation from the valence-matching principle and are not listed here. If experimental results suggest that short-range order in addition to that indicated in Table 7 is present, such arrangements can be investigated further *via* the approach used here.

TABLE 8. BOND-VALENCE TABLES FOR DISTINCT SHORT-RANGE ARRANGEMENTS IN SODIC-CALCIC AMPHIBOLES

Taramite: arrangement (2)

	M(1)	*M*(2)	*M*(3)	*M*(4)	*A*	*T*(1)	*T*(2)	Σ
O(1)	$0.33^{\times2}\downarrow$	$0.40^{\times2}\downarrow$	$0.33^{\times4}\downarrow$			1.00		2.06
O(2)	$0.33^{\times2}\downarrow$	$0.50^{\times2}\downarrow$		$0.14^{\times2}\downarrow$			1.05	2.02
O(3)	$0.34^{\times2}\downarrow\rightarrow$		$0.34^{\times2}\downarrow$					1.02
O(4)		$0.60^{\times2}\downarrow$		$0.20^{\times2}\downarrow$			1.10	1.90
O(5)				$0.05^{\times2}\downarrow$	–	1.05	0.95	2.05
O(6)				$0.11^{\times2}\downarrow$	–	1.02	0.90	2.03
O(7)					$\rightarrow$/$0.21^{\times2}\downarrow$	$0.93^{\times2}\rightarrow$		2.07
Σ	2.00	3.00	2.00	1.00	–	4.00	4.00	

Katophorite: arrangement (2)

	M(1)	*M*(2)	*M*(3)	*M*(4)	*A*	*T*(1)	*T*(2)	Σ
O(1)	$0.33^{\times2}\downarrow$	$0.27^{\times2}\downarrow$	$0.33^{\times4}\downarrow$			1.15		2.08
O(2)	$0.33^{\times2}\downarrow$	$0.33^{\times2}\downarrow$		$0.28^{\times2}\downarrow$			1.15	2.09
O(3)	$0.34^{\times2}\downarrow\rightarrow$		$0.34^{\times2}\downarrow$					1.02
O(4)		$0.40^{\times2}\downarrow$		$0.35^{\times2}\downarrow$			1.15	1.90
O(5)				$0.14^{\times2}\downarrow$	$0.15^{\times2}\downarrow$	0.96	0.85	2.10
O(6)				$0.23^{\times2}\downarrow$	$0.10^{\times2}\downarrow$	0.97	0.85	2.15
O(7)					$0.25^{\times2}\downarrow$	$0.92^{\times2}\rightarrow$		2.09
Σ	2.00	2.00	2.00	2.00	1.00	4.00	4.00	

CONCLUSIONS

The optimum patterns of short-range order of heterovalent cations in end-member amphibole compositions have been derived using the valence-matching principle of bond-valence theory. In general, there is a small number, usually two or three, of optimum patterns of short-range order that agree well with the valence-matching principle, and other postulated patterns deviate considerably from this principle. These patterns of order should prove useful in the interpretation of experimental results that are affected by short-range order (*e.g.*, infrared spectroscopy in the principal OH-stretching region, MAS NMR, EXAFS) and in the consideration of configurational entropy arguments and the development of activity models for amphiboles. These patterns of order also suggest a reason for the rarity or absence of some compositions in natural amphiboles. In end-members with one or more *local* patterns of order that deviate significantly from the valence-matching principle, that pattern may not be stable within the structure, and hence natural compositions may not be able to approach the end-member composition. Thus, for example, one of the local arrangements in tschermakite departs significantly more from the valence-matching principle than the other arrangements; this deviant arrangement is not present in hornblende, perhaps accounting for the fact that amphiboles have been synthesized only up to hornblende along the tremolite–tschermakite join (Jenkins 1994), and the observation that natural amphiboles close to tschermakite are rare or nonexistent.

ACKNOWLEDGEMENTS

I thank Roberta Oberti and Mark Welch for reviewing this manuscript and suggesting that it be a little less cryptic. This work was done during the tenure of a Visiting Professorship at CNR–CSCC, Pavia, and was supported by CNR and by the Natural Sciences and Engineering Research Council of Canada. I am extremely grateful for the opportunity to work with the CNR–CSCC staff; it was an inspiring experience.

REFERENCES

BOCCHIO, R., UNGARETTI, L. & ROSSI, G. (1978): Crystal chemical study of eclogitic amphiboles from Alpe Arami, Lepontine Alps, southern Switzerland. *Rend. Soc. It. Mineral. Petrol.* **34**, 453-469.

BROWN, I.D. (1981): The bond-valence method: an empirical approach to chemical structure and bonding. *In* Structure and Bonding in Crystals II (M. O'Keeffe and A. Navrotsky, eds.). Academic Press, New York, N.Y. (1-30).

_____ (1992): Chemical and steric constraints in inorganic solids. *Acta Crystallogr.* **B48**, 553-572.

_____ & ALTERMATT, D. (1985): Bond-valence parameters obtained from a systematic analysis of the inorganic crystal structure database. *Acta Crystallogr.* **B41**, 244-247.

_____ & SHANNON, R.D. (1973): Empirical bond-strength – bond-length curves for oxides. *Acta Crystallogr.* **A29**, 266-282.

BURDETT, J.K. & HAWTHORNE, F.C. (1993): An orbital approach to the theory of bond valence. *Am. Mineral.* **78**, 884-892.

BURNS, P.C., COOPER, M.A. & HAWTHORNE, F.C. (1994): Jahn–Teller-distorted $Mn^{3+}O_6$ octahedra in fredrikssonite, the fourth polymorph of $Mg_2Mn^{3+}(BO_3)O_2$. *Can. Mineral.* **32**, 397-403.

CAMERON, M., SUENO, S., PAPIKE, J.J. & PREWITT, C.T. (1983): High-temperature crystal chemistry of K and Na fluor-richterites. *Am. Mineral.* **68**, 924-943.

DELLA VENTURA, G. (1992): Recent developments in the synthesis and characterization of amphiboles. Synthesis and crystal-chemistry of richterites. *Trends in Mineral.* **1**, 153-192.

_____, ROBERT, J.-L., HAWTHORNE, F.C. & PROST, R. (1996a): Short-range disorder of Si and Ti in the tetrahedral double-chain unit of synthetic Ti-bearing potassium-richterite. *Am. Mineral.* **81**, 56-60.

_____, _____ & _____ (1996b): Infrared spectroscopy of synthetic (Ni,Mg,Co)-potassium-richterite. *In* Mineral Spectroscopy: a Tribute to Roger G. Burns (M.D. Dyar, C. McCammon & M.W. Schaeffer, eds.). *Geochem. Soc., Spec. Publ.* **5**, 55-63.

_____, _____, _____, WELCH, M.D. & RAUDSEPP, M. (1996c): Contrasting [6]Al ordering in synthetic Mg- and Co-pargasite. *Eur. J. Mineral.* (submitted).

_____, _____, _____, _____ & _____ (1996d): Short-range order in amphiboles synthesized along the richterite-pargasite join. *Eur. J. Mineral.* (submitted).

GRAHAM, C.M. & NAVROTSKY, A. (1986): Thermochemistry of the tremolite–edenite using fluorine analogues, and applications to amphibole – plagioclase – quartz equilibria. *Contrib. Mineral. Petrol.* **93**, 18-32.

HAFNER, S.S. & GHOSE, S. (1971): Iron and magnesium distribution in cummingtonites $(Fe,Mg)_7Si_8O_{22}(OH)_2$. *Z. Kristallogr.* **133**, 301-326.

HAWTHORNE, F.C. (1976): The crystal chemistry of the amphiboles. V. The structure and chemistry of arfvedsonite. *Can. Mineral.* **14**, 346-356.

_____ (1981a): Crystal chemistry of the amphiboles. *Rev. Mineral.* **9A**, 1-102.

_____ (1981b): Amphibole spectroscopy. *Rev. Mineral.* **9A**, 103-139.

_____ (1983): The crystal chemistry of the amphiboles. *Can. Mineral.* **21**, 173-480.

_____ (1995): Entropy-driven disorder in end-member amphiboles. *Can. Mineral.* **33**, 1189-1204.

_____ (1996): Structural mechanisms for light-element variations in tourmaline. *Can. Mineral.* **34**, 123-132.

_____, DELLA VENTURA, G. & ROBERT, J.-L. (1996b): Short-range order of (Na,K) and Al in tremolite: an infrared study. *Am. Mineral.* **81**, 782-784.

_____, _____ & _____ (1996c): Short-range order and long-range in amphiboles: a model for the interpretation of infrared spectra in the principal OH-stretching region. *In* Mineral Spectroscopy: a Tribute to Roger G. Burns (M.D. Dyar, C. McCammon & M.W. Schaeffer, eds.) *Geochem. Soc., Spec. Publ.* **5**, 49-54.

_____ & GRUNDY, H.D. (1978): The crystal chemistry of the amphiboles. VII. The crystal structure and site-chemistry of potassian-ferri-taramite. *Can. Mineral.* **16**, 53-62.

_____, OBERTI, R., CANNILLO, E., SARDONE, N., ZANETTI, A., GRICE, J.D. & ASHLEY, P.M. (1995): A new anhydrous amphibole from the Hoskins mine, Grenfell, New South Wales, Australia: description and crystal structure of ungarettiite, $NaNa_2(Mn^{2+}{}_2Mn^{3+}{}_3)Si_8O_{22}O_2$. *Am. Mineral.* **80**, 165-172.

_____, _____ & SARDONE, N. (1996a): Ordering at the *A* site in clinoamphiboles: the effects of composition on patterns of order. *Can. Mineral.* **34**, 577-593.

_____, _____, UNGARETTI, L. & GRICE, J.D. (1992): Leakeite, $NaNa_2(Mg_2Fe^{3+}{}_2Li)Si_8O_{22}(OH)_2$, a new alkali amphibole from the Kajlidongri manganese mine, Jhabua district, Madhya Pradesh, India. *Am. Mineral.* **77**, 1112-1115.

_____, _____, _____ & _____ (1996d): A new hyper-calcic amphibole with Ca at the A site: fluor-cannilloite from Pargas, Finland. *Am. Mineral.* **81**, 995-1002.

_____, UNGARETTI, L., OBERTI, R., BOTTAZZI, P. & CZAMANSKE, G.K. (1993b): Li: an important component in igneous alkali amphiboles. *Am. Mineral.* **78**, 733-745.

_____, _____, _____, CANNILLO, E. & SMELIK, E.A. (1994): The mechanism of [6]Li incorporation in amphiboles. *Am. Mineral.* **79**, 443-451.

_____, _____, _____, CAUCIA, F. & CALLEGARI, A. (1993a): The crystal chemistry of staurolite. I. Crystal structure and site populations. *Can. Mineral.* **31**, 551-582.

JAHN, H.A. & TELLER, E. (1937): Stability of polyatomic molecules in degenerate electronic states. I. Orbital degeneracy. *Proc. R. Soc.* **A161**, 220-235.

JENKINS, D.M. (1988): Experimental study of the join tremolite–tschermakite. A reinvestigation. *Contrib. Mineral. Petrol.* **99**, 392-400.

_____ (1994): Experimental reversal of the aluminum content in tremolitic amphiboles in the system H_2O–CaO–MgO–Al_2O_3–SiO_2. *Am. J. Sci.* **294**, 593-620.

LAW, A.D. (1976): A model for the investigation of hydroxyl spectra of amphiboles. *In* The Physics and Chemistry of Minerals and Rocks (R.G.J. Strens, ed.) J. Wiley & Sons, London, U.K. (677-686).

OBERTI, R., HAWTHORNE, F.C., UNGARETTI, L. & CANNILLO, E. (1995a): $^{[6]}$Al disorder in amphiboles from mantle peridotites. *Can. Mineral.* **33**, 867-878.

_____, UNGARETTI, L., CANNILLO, E., HAWTHORNE, F.C. & MEMMI, I. (1995b): Temperature-dependent Al order–disorder in the tetrahedral double-chain of *C2/m* amphiboles. *Eur. J. Mineral.* **7**, 1049-1063.

PAPIKE, J.J. & CLARK, J.R. (1968): The crystal-structure and cation distribution of glaucophane. *Am. Mineral.* **53**, 1156-1173.

_____, ROSS, M. & CLARK, J.R. (1969): Crystal-chemical characterization of clinoamphiboles based on five new structure refinements. *Mineral Soc. Am., Spec. Pap.* **2**, 117-136.

PAULING, L. (1929): The principles determining the structure of complex ionic crystals. *Am. Chem. Soc. J.* **51**, 1010-1026.

PAWLEY, A.R., GRAHAM, C.M. & NAVROTSKY, A. (1993): Tremolite–richterite amphiboles: synthesis, compositional and structural characterization, and thermochemistry. *Am. Mineral.* **78**, 23-35.

ROBINSON, K., GIBBS, G.V., RIBBE, P.H. & HALL, M.R. (1973): Cation distribution in three hornblendes. *Am. J. Sci.* **273A**, 522-535.

SEIFERT, F. (1978): Equilibrium Mg–Fe^{2+} cation distribution in anthophyllite. *Am. J. Sci.* **278**, 1323-1333.

SHANNON, R.D. (1976): Revised effective ionic radii and systematic studies of interatomic distances in halides and chalcogenides. *Acta Crystallogr.* **A32**, 751-767.

SMELIK, E.A., JENKINS, D.M. & NAVROTSKY, A. (1994): A calorimetric study of synthetic amphiboles along the tremolite–tschermakite join and the heats of formation of magnesiohornblende and tschermakite. *Am. Mineral.* **79**, 1110-1122.

STRENS, R.G.J. (1966): Infrared study of cation ordering and clustering in some (Fe,Mg) amphibole solid solutions. *Chem. Comm. (Chem. Soc. London)* **15**, 519-520.

_____ (1974): The common chain, ribbon, and ring silicates. *In* The Infrared Spectra of Minerals (V.C. Farmer, ed.). *Mineral. Soc., Monogr.* **4**, 305-330.

WELCH, M.D., KOLODZIEJSKI, W. & KLINOWSKI, J. (1994): A multinuclear NMR study of synthetic pargasite. *Am. Mineral.* **79**, 261-268

Received December 6, 1995, revised manuscript accepted December 17, 1996.